ISSN 1070-3284, Russian Journal of Coordination Chemistry, 2009, Vol. 35, No. 8, pp. 553–565. © Pleiades Publishing, Ltd., 2009.
Original Russian Text © V. I. Sokolov, 2009, published in Koordinatsionnaya Khimiya, 2009, Vol. 35, No. 8, pp. 563–575.

Chiral Stereochemistry of Nanoparticles

V. I. Sokolov

Nesmeyanov Institute of Organoelement Compounds, Russian Academy of Sciences, ul. Vavilova 28, Moscow, 119991 Russia

E-mail: sokol@ineos.ac.ru

Received February 2, 2008

Abstract—The whole array of organic and inorganic nanoparticles, from fullerenes and carbon nanotubes to metals and metal oxides, is discussed in terms of chirality and its stereochemical consequences on the basis of the unified "core–shell" concept.

DOI: 10.1134/S1070328409080016

INTRODUCTION

In the world of molecular objects, including macromolecular ones, chirality inevitably gives rise to optical activity. Furthermore, this holds for regular crystals as well.

In the world of nanoparticles, the situation is ambiguous. First of all, this ambiguity is associated with a variety of nanoobjects themselves. According to a canonical definition [1–4], nanoparticles are objects 1 to 100 nm in size. However, this definition does not specify their structures. When comparing various classes of nanoparticles, one can conclude that the dimensional criterion should be supplemented with a structural one. Generally speaking, nanoparticles consist of the central core surrounded by attached ligands/addends, which stabilize the whole structure.[1] The absence of ligands/addends is a specific, very uncommon case; the exception is a molecular form (fullerenes).

Using such an approach, one can consider in a unified manner all nanoparticles, from fullerenes and carbon nanotubes to nanometals and nanooxides, from the viewpoint of chiral stereochemistry. The main tool of chiral stereochemistry is circular dichroism (CD). Note that classic circular dichroism in the UV-VIS range [5] generally corresponds to electron transitions in the cores of nanoparticles and to electron transfers between ligands/addends and the core, while circular dichroism in the IR range, which came into practice in the 1980s after relevant instruments had been designed [6, 7], reflects the chiral situation mainly in ligands/addends and partially between them and the core.

A detailed consideration of the structures and behavior of nanoparticles reveals an important difference between organic (based on carbon, ONPs) and inorganic nanoparticles (based on other elements, INPs).

Nanocarbon conceptually differs from other nanoparticles much as organic chemistry differs from inorganic chemistry. These differences arise from the ability of carbon atoms to (1) exist in different hybridization states and (2) form chains and clusters of covalently bonded atoms. The schematic diagram describing a diversity of nanocarbon forms was proposed in [8] and is shown below with a slight modification:

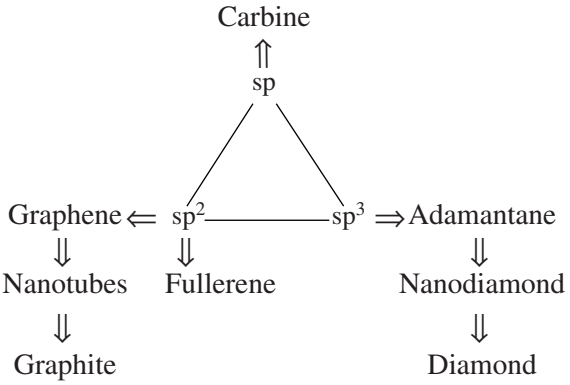

Adamantane is included in the scheme as a molecular precursor of the unit cell framework of diamond. It should be noted that only nanocarbon can generate the sole simple molecular species (fullerenes) in the whole nanochemistry. Because of this, they are very stable without any addends. All other "molecular" forms are actually intermolecular complexes that can substan-

[1] Conventionally, ligands are molecules or ions attached to a metal atom and addends are those attached to a carbon atom, without specifying the nature of bonding. In most cases, ligands are more labile with respect to the core than are addends. An array of ligands makes a shell around the core, so-called a coordination sphere. Addends differ from ligands only by their σ-bonding, which is of no importance in this case.

tially exceed the aforesaid dimension limits, especially complexes of biomolecules.

Carbon nanoparticles are an extension of polycarbon molecules to the nanolevel. They contain double "olefinic" bonds whose reactivity is enhanced by geometrical strain; in addition, these particles are characterized by high electron-withdrawing properties and high hydrophobicity. This holds for both individual fullerene molecules and polymeric carbon nanotubes. Direct experiments revealed the presence of double bonds even on the diamond (especially, nanodiamond) surface [9], which is responsible for the high adsorption properties of nanodiamonds.

Thus, carbon nanoparticles contain structural elements inherent in simpler organic molecules. Because of this, the role of chemistry in the study of nanocarbon structures is more important than for other nanoparticles since the main reactivity paradigms have been already developed in classic organic chemistry. Nevertheless, strained double bonds in fullerenes and nanotubes can enter into novel, previously unknown reactions, which has enriched both organic and organometallic chemistry.

Another difference between organic and inorganic nanoparticles is in the design concept: in solution (so-called bottom-up technique), INPs form by agglutination (i.e., every next particle "adheres" to an already formed conglomerate of similar particles), while ONPs are closer to the inflexional type: every unit has its specific properties and changes (inflexions) in a formed object are made by addition of any groups (addends/ligands). Strictly speaking, the agglutination of ONPs occurs during their formation from the carbon vapor.

In inorganic nanoparticles (metals, metal oxides, metal sulfides, etc.), the core is usually surrounded by a ligand shell. It should be emphasized that the outer layer of the central core of a nanoparticle is more significant than its size. The properties of the outer layer are decisive for the nature and geometry of the ligand shell, which compensates for the free valences of surface atoms. As the result, the particles become more stable and can pass into a solvent appropriate to the ligand nature. For instance, hydrophilic ligands make the nanoparticles more soluble in water, which is desirable for their application. The resulting colloidal solution contains only a (not always dominant) fraction of the "major" compound. However, this compound can influence some properties of the whole solution (e.g., when ligands are unresponsive in a certain spectral region or, in contrast, they specifically interact with the core).

The main goal of this review was to consider the consequences of the chirality of various nanoparticles; other structural aspects of nanoparticles will be only mentioned, if necessary. It is of stereochemical interest that some symmetric electron transitions in an asymmetric environment can become optically active, giving rise to the corresponding Cotton effects (CEs) in CD spectra. This phenomenon in organic and coordination chemistry is called induced circular dichroism (ICD) and also takes place in both organic and inorganic nanoparticles. Fullerene derivatives constitute a particular group: the sole form of molecular nanoparticles.

Unlike true CD, magnetic circular dichroism, to which much more studies of nanoparticles are devoted, has nothing to do with chirality. Magnetic circular dichroism is known [10] to occur in all (including achiral) molecules and objects, so it is beyond the scope of this review.

The general principles of the chirality of nanoobjects regarded as a central core with attached ligands/addends remain the same as described in the review of the stereochemistry of fullerenes [11] containing an ellipsoidal carbon core. Nanotubes have cylindrical carbon (or different) cores; inorganic nanoparticles have polyhedral cores.

The chirality of an object can arise from the chirality of the core itself, the chirality of ligands/addends, and a chiral arrangement of achiral ligands/addends on the core surface. Since no other cases are possible, one can consider the chirality of all (both organic and inorganic) nanoparticles in terms of a unified approach. First we consider carbon nanoparticles, specifically fullerenes and nanotubes, because the literature data on the stereochemistry of nanodiamonds, nanoonions, and other carbon nanoobjects are lacking.

Selected parameters of two main forms of nanocarbon (fullerenes and nanotubes) are compared below:

Fullerenes	Nanotubes
Individual molecules	Polymers
Poorly soluble	Insoluble
Ellipsoidal inner cavity	Cylindrical inner cavity
Capable of irreversibly entrapping atoms in their inner cavity	Capable of reversibly entrapping atoms and molecules in their inner cavity

Based on the concept of a limited similarity of fullerenes with carbon nanotubes because of the presence of strained double bonds, one can estimate how far these two classes of carbon nanostructures are similar. In the next step of generalization, the limits of the analogy between all nanoparticles can be determined.

FULLERENES

A specific dual character of fullerenes arises from the following reasons. On the one hand, they consist only of carbon atoms and hence are objects of inorganic chemistry. On the other hand, the presence of double

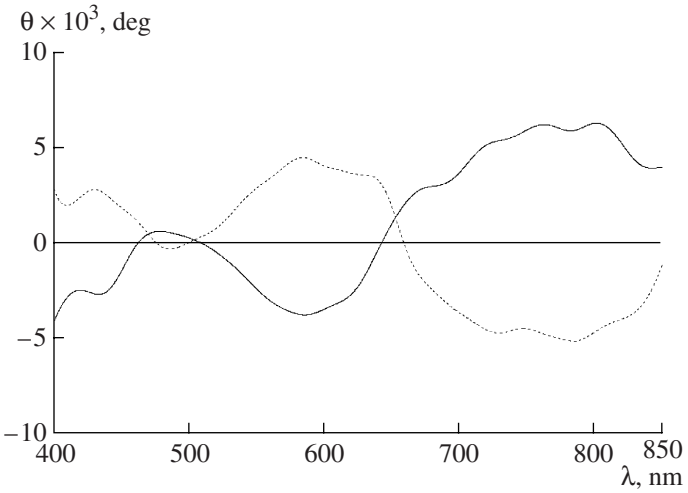

Fig. 1. CD spectra of the molybdenum complex with C_{60} and the enantiomeric N,N-ligand.

carbon–carbon bonds with their particular reactivity makes fullerenes objects of organic chemistry. One can see with this example that the bonding nature is more important than the nature of atoms in the determination of the chemical individuality of a molecule.

The chiral stereochemistry of fullerenes and early relevant studies were reviewed in [11]. In this review, we consider only the latest papers devoted to stereochemical problems. In the last few years, enantiomeric C_{76} was assigned the absolute configuration (+)589-(fC)-C_{76} [12] from theoretical calculations of CD spectra and optical rotatory dispersion [13].[2] An analysis of the CD spectra of fullerenes is complicated by the lack of theoretical detailed concepts of the nature and symmetry of electron transitions [14]. Essentially, current investigations only accumulate factual evidence and a range of experimental objects is narrow and should be extended.

All currently known fullerene derivatives are based on achiral C_{60} and C_{70}. If ICD due to electron transitions in the fullerene system is observed for optically active compounds, this dichroism is intramolecular, except for intermolecular complexes of C_{60} with γ-cyclodextrin (γ-CD). It is the latter complexes that have been extensively studied because of their solubility in water. The ICD spectrum was first measured in [15] and the stoichiometry of the complex was found to be γ-CD : C_{60} = 2 : 1 (this was done in the range below 400 nm, where the fullerene chromophore has no characteristic absorption). These results were not commented. In more recent papers, no CD spectra of fullerene complexes with cyclodextrin have been cited. Interestingly, in the study of a reaction of the above complex with BSA albumin [16], the most attractive range for ICD (above 400 nm, where only fullerene absorbs) was also ignored. This was explained by the interest of the researchers only in (!) "a possible change in the albumin conformation", for which the 190–400 nm range is informative. In this range, a change in the CD spectrum was negligible, although the isotropic UV spectrum shows a distinct band at 329 nm due to C_{60}. Therefore, it does not become optically active in the hybrid BSA-C_{60}. The ICD observed for optically active poly(phenylacetylenes) with pendant C_{60} substituents is probably due to the helical structure of a certain sign. The spectrum contains several CEs on fullerene chromophores, which are especially intense at long wavelengths: a (–) doublet at ~675 nm and a (+) singlet at ~710 nm [17].

Metal complexes with fullerenes are usually stable when they contain enantiomeric P-ligands. We obtained complexes of η^2-C_{60} with palladium, platinum, and the optically active ligand (+)-DIOP bearing two chiral carbon centers [18, 19] and examined their CD spectra. An analogous study with the ligand (–)-DIOP carried out a few years later [20] revealed nothing new for the description of the chiroptical properties of these complexes [21]. The resulting molybdenum and tungsten complexes $C_{60}M[(–)DIOP](CO)_3$ show CEs. Mirror curves in the CD spectrum (Fig. 1) were obtained in [22] for a rare type of C_{60} complexes with an enantiomeric N,N-ligand to the molybdenum atom, $(\eta^2$-$C_{60})MoL^*(CO)_3$:

[2] In the Schlegel diagram, (fC) means clockwise and (fA) means anticlockwise.

L* = 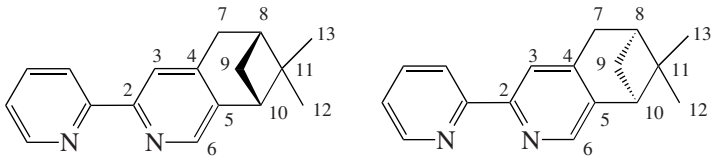

Later, axially chiral palladium complexes with C_{60} or C_{70} and phosphine ligands of the bithienyl series were obtained [23].

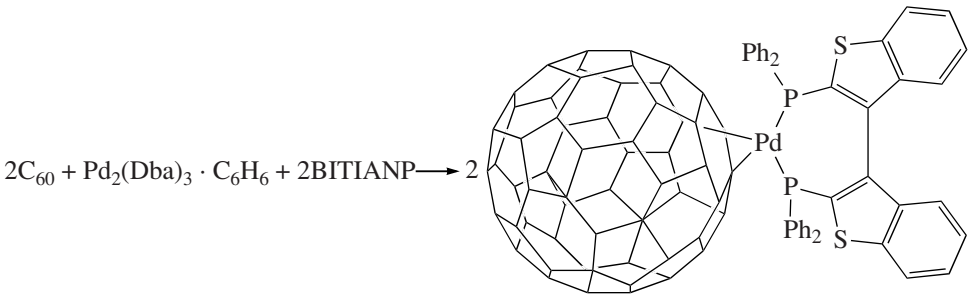

The CD spectra of palladium complexes with C_{60} and C_{70} and the axially chiral ligand BITIANP are shown in Fig. 2. In the spectra, the CE due to the fullerene absorption for the complex with C_{70} is shifted to the longer wavelengths compared to the complex with C_{60}.

To study the influence of planar chirality on the fullerene chromophore, a N-methylpyrroli-

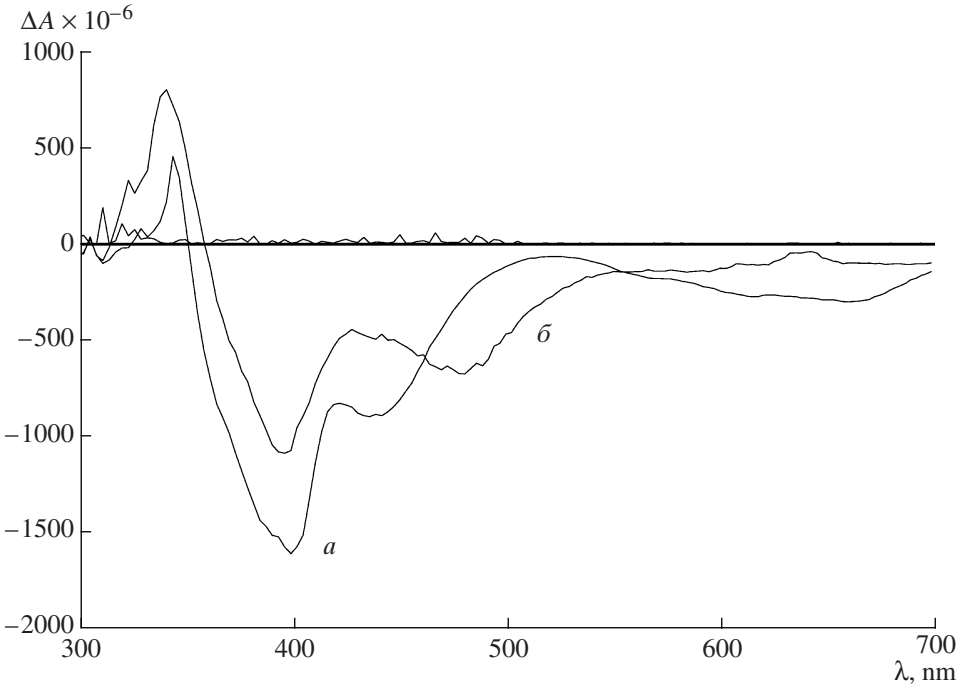

Fig. 2. CD spectra of the palladium complexes (a) η^2-C_{60})Pd[(–)-BITIANP] and (b) (η^2-C_{70})Pd[(–)-BITIANP] with the axially chiral enantiomeric P,P-ligand.

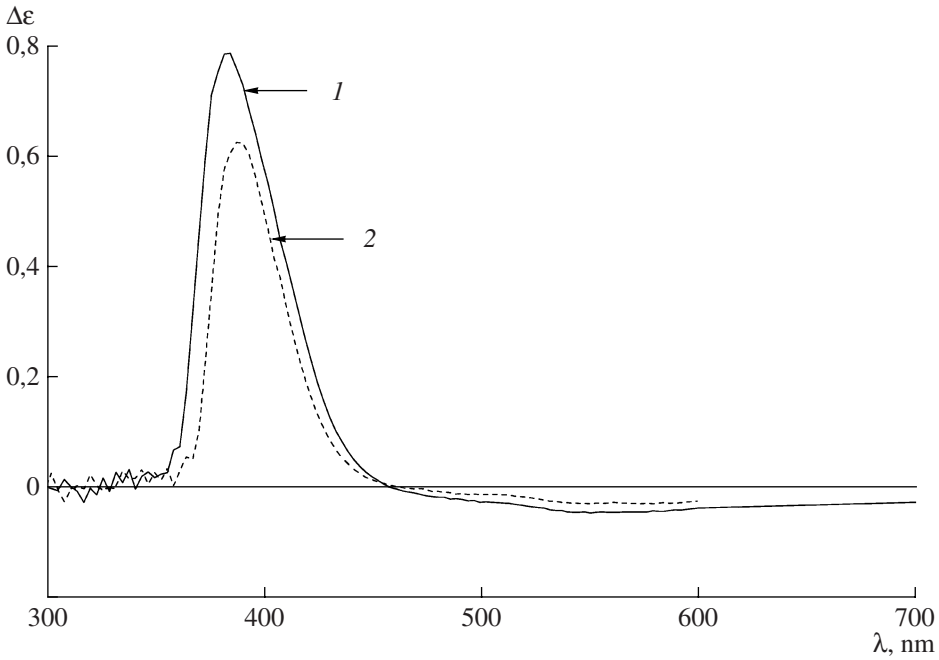

Fig. 3. CD spectra of planar-chiral (*1*) β-bicymantrenyl aldehyde and (*2*) the Schiff base.

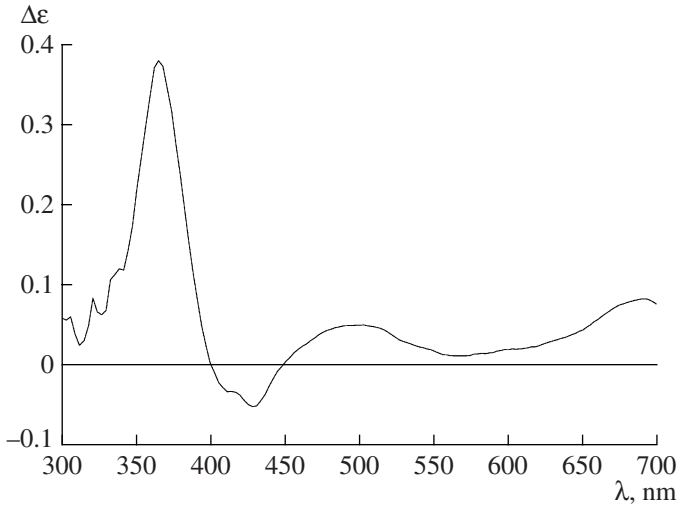

Fig. 4. CD spectrum of 2-bicymantrenyl-N-methylpyrrolidino[60]fullerene.

dino[60]fullerene derivative containing enantiomeric β-bicymantrenyl in position 2 of the heterocycle was used as a different structural model [24]. This derivative was obtained by the Prato reaction from prepared optically active planar-chiral β-bicymantrenyl aldehyde [25, 26]. In the CD spectra of the aldehyde and the Schiff base (Fig. 3), an intense positive CE due to the bicymantrenyl chromophore appears at 384–387 nm. The CD spectrum of 2-bicymantrenyl-N-methylpyrrolidino[60]fullerene shows several CEs (Fig. 4). The positive CE due to the separate bicymantrenyl chromophore is shifted to the shorter wavelengths (367 nm), probably because of the electron-withdrawing effect of the fullerene. Two negative and one positive CE at 400–550 nm can be assigned to an electron transfer from the ligand to fullerene. The positive CEs due to the fullerene core appear at the longer wavelengths [27]. It is interesting to compare the positions of the CEs with those in the CD spectrum of a unique representative of the cymantrene series, namely, the enantiomeric free radical (2-carboxymethyl-1-methyl)cyclopentadienylmanganese(phenylthiodicarbonyl) [28]: 347 and ~480 nm; the latter CE is in the range characteristic of the intramolecular electron transfer.

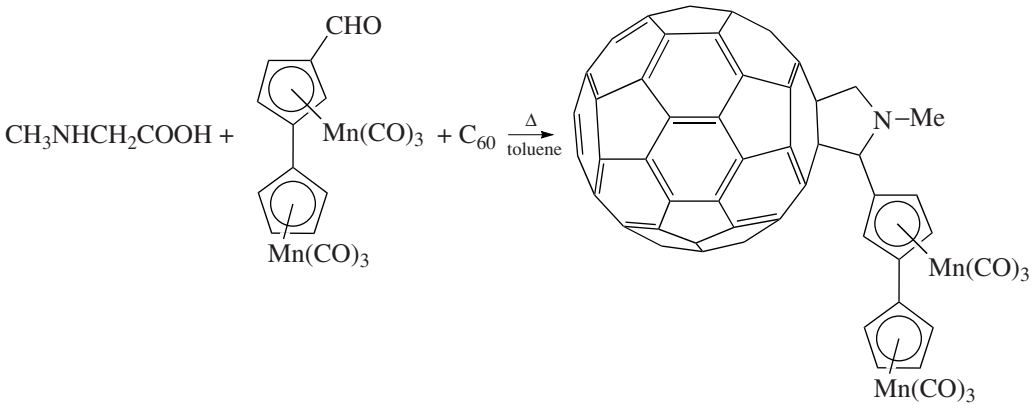

CARBON NANOTUBES

Carbon nanotubes (CNTs) are divided into single-walled (SWNTs), double-walled (DWNTs), or multi-walled ones (MWNTs) [29–31]. All of them are virtually insoluble in any solvent, though sufficiently short nanotubes in the presence of surfactants can form colloidal solutions. The solubility can be enhanced by addition of appropriate functional groups.

Single-walled carbon nanotubes can be imagined as a rolled graphene sheet (a one-atom-thick sheet of graphite). The symmetry of a nanotube varies with the angle between the rolling line and the axis of the resulting CNT (Fig. 5). A nanotube can be chiral or achiral. Since the catalytic formation of a CNT cannot yet be controlled, the resulting mixture consists of chiral or achiral nanotubes and the tube cannot be checked for chirality during the synthesis.

If a graphene sheet is rolled into a cylindrical tube in such a way that part of the edges of the hexagons are parallel (**A**) or perpendicular to the tube axis (**B**), then the resulting nanotube will be achiral (symmetry group D_{nd}). The former version of rolling is referred to as "zigzag" and the latter, as "armchair", because of resembling patterns of the edge line upon cutting (Fig. 6).

Because each hexagon contains three localized double bonds, one of them is inevitably parallel (**A**) or perpendicular to the tube axis (**B**), while the other two make with it an angle of about 60°. If addition of a complexed metal (or the Prato reaction, or something else) occurs at one of the double bonds, then the resulting structure will be chiral (group C_1) with a probability of 2/3 and achiral (group C_s) with a probability of only 1/3. The latter structure retains the plane of symmetry passing through the ex-double bond involved in the addition reaction. Thus, achiral nanotubes can produce chiral derivatives. Moreover, if an addend contains an enantiomeric group, this derivative can undergo resolution into enantiomers before the achiral nanotube. Accordingly, chiral nanotubes can likewise generate diastereomeric derivatives via introduction of a new chirality element.

All other types of rolling of a graphene sheet that are inside the dashed angle in Fig. 5 (i.e., intermediate structures between the zigzag and armchair configura-

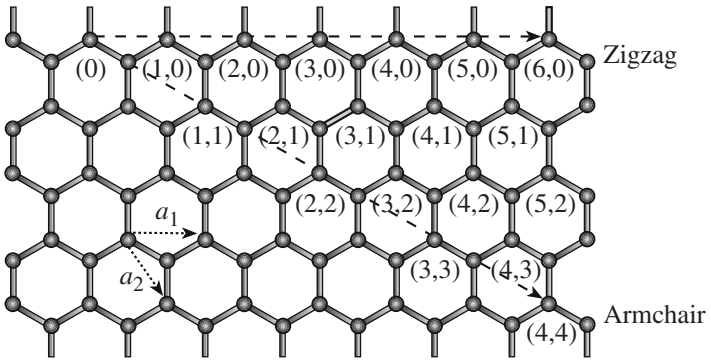

Fig. 5. Scheme of rolling of a graphene sheet into various carbon nanotubes.

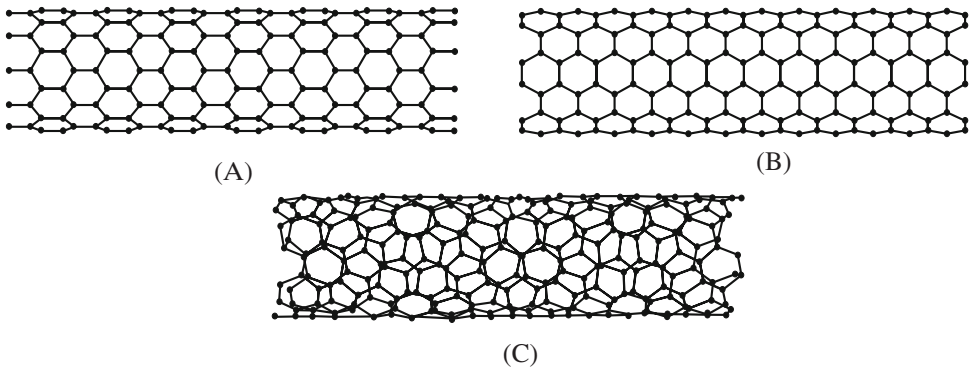

Fig. 6. Types of carbon nanotubes: achiral tubes with the zigzag (**A**), armchair configurations (**B**), and chiral tubes (**C**).

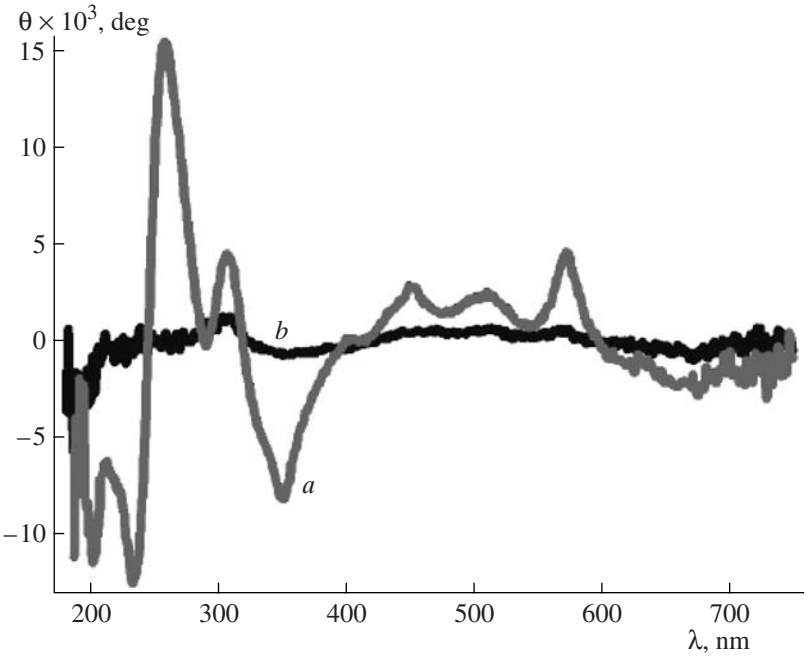

Fig. 7. CD spectra of (a) a supramolecular complex (a DNA analog) and (b) a single-walled carbon nanotube (SWNT).

tions) produce chiral nanotubes represented by structure **C**. This angle called chiral nanotube angle is 0° for zigzag tubes (**A**), 30° for armchair tubes (**B**), and intermediate between 0° and 30° for chiral nanotubes (**C**). Carbon nanotubes are characterized by a two-digit index written as (*n*, 0) for (**A**), (*n, n*) for (**B**), and (*n, m*) for (***C***), $n \neq m$. Useful information, including the tables of indices and the corresponding geometrical parameters of CNTs, can be found in [32]. Carbon nanotubes can be semiconductors or metals. Metallic conductivity is exhibited by ca. 33% of nanotubes (including all armchair tubes of the type **B**).

The first ICD of single-walled CNTs was observed in 2006 [33], when racemic tubes were "wrapped" in DNA (or more specifically, in its synthetic analog oligomer $d(GT)_{20}$) in D_2O in the presence of sodium dodecylbenzenesulfonate. When $d(GT)_{20}$ was removed from the solution without making any other changes, the Cotton effects disappeared; therefore, the induction is due to the electron transitions in CNTs (Fig. 7).

An experimental approach to the synthesis of enantiomer-enriched CNTs was developed in 2007. The enrichment was achieved by fractional distillation of a supramolecular complex of a nanotube with diporphyrin containing several identical enantiomeric *meso*-substituents [34]. Two porphyrin moieties are linked by a *meta*-phenylene spacer to form something like nanotweezers that seize a nanotube by means of aryl–aryl interactions:

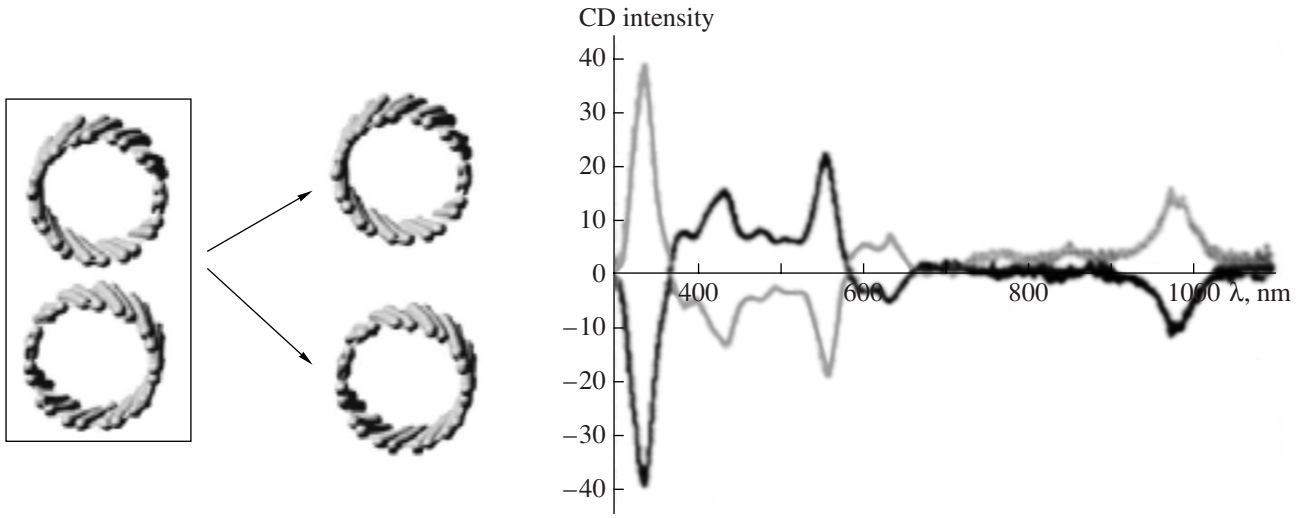

Fig. 8. CD spectra of both enantiomers of resolved carbon nanotubes.

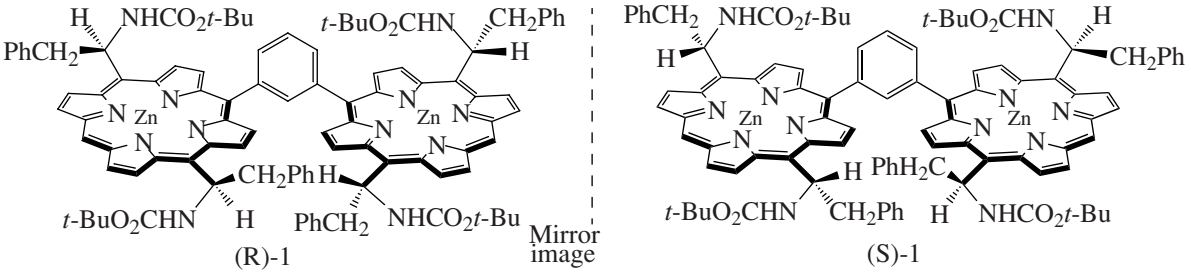

Partial resolution of nanotubes into enantiomers was convincingly proved in [35] by observing mirror-image curves of both enantiomers in the CD spectrum showing no less than ten CEs of opposite signs, which were tentatively assigned to chiral CNTs of different sizes (Fig. 8).

INORGANIC NANOPARTICLES

A considerable part of inorganic nanoparticles are metal ones. A specific situation arises: the chemistry of molecular metal clusters with organic ligands has been developed for a long period of time. In some cases, their structures were characterized by X-ray diffraction analysis for sufficiently great numbers of atoms (e.g., Au_{55} [36] or Pd_{145} [37]).

The border zone between molecular metal clusters and nanoparticles include objects with not well defined structures (so-called fuzzy zone). Indeed, it is very difficult to estimate variations in the number of atoms in a molecular object when its properties remain virtually unchanged, as with polynuclear metal clusters. An objective estimation of the nanoparticle sizes is complicated. Almost all techniques are indirect and provide an estimate interval, except for X-ray diffraction analysis (but this technique is suitable for molecular crystals only). In [38], an analogy between polymer homologs and the positive integer series was drawn: with an increase in N, the difference between the adjacent members N and $N + 1$ of the series becomes less and less appreciable. In the fullerene series, the difference between individual members is mainly due to the changed group of symmetry, while among nanotubes of finite length, due to a distance from a particular site to the end. According to data for gold clusters [39], their samples are a mixture of related clusters with a sufficiently narrow distribution of compositions.

A great part of numerous studies of separate groups of inorganic nanoparticles, their synthesis, and their spectroscopic and other properties have been generalized in [39–41]. Unfortunately, chirality and optical activity are poorly presented in those monographs and reviews. Indeed, this subject has received attention only recently because of its complexity and synthetic problems associated with the preparation of models. However, it should be recollected that chirality is not optical activity but only its prerequisite.[3]

[3] A search in the Internet finds a great number of references to "optically active nanoparticles" but the overwhelming majority of them have nothing to do with optical activity in the stereochemical sense.

In the aforesaid analysis of chirality, we point to three sources of chirality for any nanoparticles. This trivial conclusion was detailed for inorganic nanoparticles by several teams of researchers. Calculations performed in 1996 predicted [42], and experiments carried out two years later demonstrated [43], that "bare" (ligand-free) Ni_{39} clusters prefer a chiral structure of lower symmetry to an achiral structure of higher symmetry. This relates to ligand-free Au_{28} or Au_{55} clusters [44] and similar structures [45] and is believed to be a general rule. Another team of researchers [46] reported that optical activity can arise from perturbation of an achiral metal core by a chiral organic shell (this could be predicted *a priori* from general considerations), though saying nothing of the intensity of this effect. The accuracy of the calculations against experimental data is also unknown.

Among nanometals, nanogold complexes with thiol ligands are best studied because of their stability and easy formation: this is due to an exceptional thiophilicity of gold and its known tendency toward homoclustering. A preferred route to these complexes involves the reduction of $HAuCl_4$ in a two-phase liquid–liquid system [47].

The optical activity of the Au_{28} nanocluster with the chiral tripeptide L-glutathione (γ-L-Glu-L-Cys-Glu) as a ligand seemed to be observed for the first time in the UV-VIS range in [48]. After the separation of the mixture of products by gel electrophoresis, three smaller clusters (4–8 kD) showed strong optical activity comparable in CE with higher helicenes or chiral fullerenes [49].

Nanoparticles with such stabilizing thiols as N-acetyl-L-cysteine [50], N-isobutyryl-L-cysteine [51], penicillamine[4] [52], and 1,1'-dinaphthyl-2,2'-dithiol [53] were also obtained. In [52], gold nanoparticles covered with penicillamine enantiomers were separated by gel electrophoresis into three fractions containing 6, 50, and 150 gold atoms. According to their CD spectra (mirror-image curves with different enantiomers of the amine), the anisotropy factor decreases with an increase in the size of the nanoparticle (Fig. 9). A combination of the thiol and carboxyl functions in the ligand molecule seems to be optimal because the former attaches the ligand to the core, while the latter makes it soluble in water.

For the aforesaid reasons, the sole example of a water-soluble, crystalline nanometal complex characterized by high-resolution (1.1 Å) X-ray diffraction analysis was $Au_{102}(SR)_{44}$, where R = *p*-carboxyphenyl [54]. Although these crystals were obtained from zerovalent colloidal gold and *n*-mercaptobenzoic acid, the resulting product is a classic cluster composed of a positively charged polymetal core and many thiolate anions. The behavior of the thiol protons remains unclear, which was also noted in [54]. The species SR interact with gold and with each other by hydrogen bonding to form a rigid outer layer. The particles are chiral and both enantiomers alternate in the crystal lattice. Originally, the researchers [54] attributed the discrete nature of the particles to the formation of a stable 58-electron shell and packing of the central gold atoms in a highly symmetrical 49-atom Marks decahedron [55], the chirality of the particle arising from the effect of the ligands on the outer-layer gold atoms.

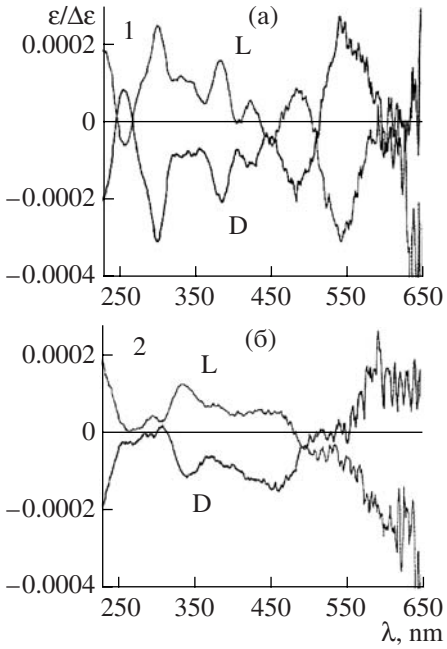

Fig. 9. Comparison of the anisotropy factors (ε/Δε) in the CD spectra of fractions (a) 1 and (b) 2 of gold nanoclusters (isolated by gel-permeation chromatography) with the L- and D-enantiomers of penicillamine as ligands.

In addition, most sulfur atoms are bound to two Au atoms, thus forming stereogenic fragments. Although this cluster is a racemate, it is a structural model of related enantiomeric complexes (their exact structures are unknown) with SH-containing enantiomeric compounds instead of achiral *p*-mercaptobenzoic acid.

Later, by combined efforts of crystallographers and researchers dealing with DFT calculations [56], this model was refined with retention of the "core–shell" principle and a concept of "superatoms" was developed. This concept characterizes a compact symmetric core with a filled spherical electron shell and a large energy gap between it and the unoccupied states. The structure of $Au_{102}(p\text{-MBA})_{44}$ is best described as consisting of the metal core Au_{79} (approximate symmetry D_{5h}) with a protective gold–thiolate layer of the formula $Au_{23}(p\text{-MBA})_{44}$. Therefore, the more accurate formula of this nanoparticle is $Au_{79}[Au_{23}(p\text{-MBA})_{44}]$. The gold atoms in the cluster are in two chemical states: 79 atoms (Au_{core}) are metallic (zero charge) and 23 atoms bound to the thiolate ligands (Au_L) are oxidized.

[4] Penicillamine is a trivial name for β,β-dimethyl-L-cysteine, a metabolite of naturally occurring penicillin.

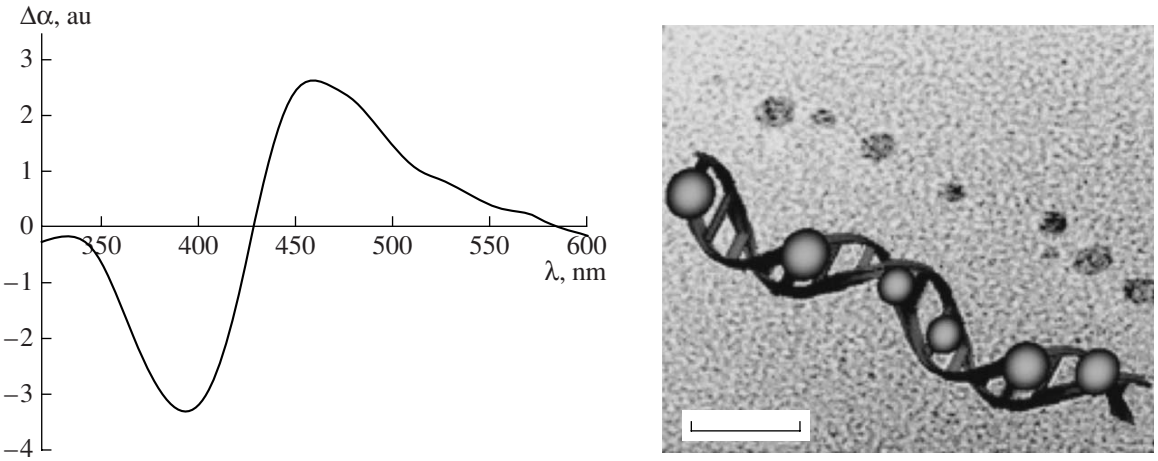

Fig. 10. CD spectrum of a silver nanocluster induced by a DNA analog.

In the last few years, the most comprehensive study of chiral gold nanoparticles stabilized by thiols was made by Bürgi and Gautier, who carried out "chiral inversion" of gold nanoparticles (i.e., complete replacement of ligands with one enantiomeric configuration in the shell by ligands with the other configuration, which gives rise to a mirror-image curve of the Cotton effect) [57]. This provided evidence that ICD is due just to the ligand chirality. Another team of researchers observed the CE after racemic penicillamine in the ligand shells of silver nanoparticles had been replaced by enantiomeric one [58].

For metal nanoparticles no smaller than 3 nm, their spectra show absorption bands due to a surface plasmon resonance.[5] Recently, chiral induction at the plasmon resonance band was reported [59]. First, silver ions were sorbed at the double-strand homopolymer (~700 base pairs) poly(dG)-poly(dC), an analog of DNA, to give a stable complex. Then they were reduced with sodium borohydride, yielding silver nanoparticles. The initial homopolymer shows a single positive CE at 260 nm, which changes into a negative CE upon the sorption of Ag^+. In the CD spectra of the reduced complex, two characteristic CEs appear in the positive and negative areas (Fig. 10), which correspond to a new peak at 425 nm in the UV spectrum. This was interpreted as chiral induction at the plasmon resonance band. Interestingly, this effect is not observed in the adsorption of silver nanoparticles prepared in solution; i.e., the double helix acts as a chirality-producing matrix during the synthesis of nanosilver. The homopolymer poly(dA)-poly(dT) behaves likewise.

Interestingly, the aforementioned enantiomeric thiols (e.g., penicillamine) can induce optical activity in quantum dots[6] of the type CdS, probably through the chiral shell, since the core remains achiral [64, 65]. For the L- and D-enantiomers of penicillamine, enantiomeric CD curves in the 200–400 nm range show alternation of the CE sign at 207, 252, 293, 320, and 345 nm. These nanoparticles are schematically depicted in Fig. 11. Their CD spectra are shown in Fig. 12. The spectral pattern does not change with the growth of nanoparticles. Cadmium sulfide nanocrystals luminesce intensely; however, no chiral polarization was detected in the emitted light (λ_{max} = 495 nm).

The use of a protein with a fixed cavity for the formation of homogeneous nanoparticles of metal sulfides (CdS, CdSe, and Au_2S) is worth noting [66–68]. Because the size of the apoferritin cavity is 7 nm, nanoparticles obtained by a slow pH-controlled reaction between the corresponding cation and anion in the presence of this protein are no larger than 6 nm. Heating over nitrogen affords single crystals. Unfortunately, no data on the chiroptical properties of metal sulfide nanoparticles embedded in the protein are available.

CONCLUSIONS

The chemistry and physics of nanoparticles attract great attention because their electromagnetic, optical, catalytic, mechanical, and other properties differ substantially from the properties of the respective compact materials and thus provide new scope for use of them in diverse fields of science and engineering. Because of this, the term "nanotechnology" has come into use before the term "nanoscience" (which should precede the former in the hierarchical sense) and is used more widely. Chiral stereochemistry is closer to optical and catalytic properties. It is known that light absorption

[5] Surface plasmon resonance is the collective vibrations of the conduction electrons in metal. The position of the absorption band depends on the size of metal nanoparticles: for gold, this band appears at 510–580 nm [60, 61].

[6] Nanosized conglomerates of metal sulfides, which are of practical interest because of their properties of semiconductors, luminophores, etc., have been called quantum dots [62, 63].

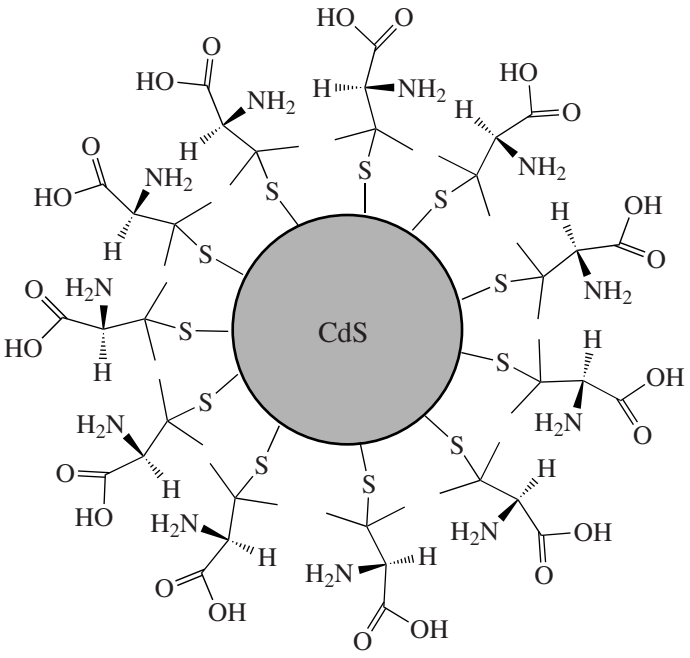

Fig. 11. Schematics of CdS nanoparticles with a ligand shell.

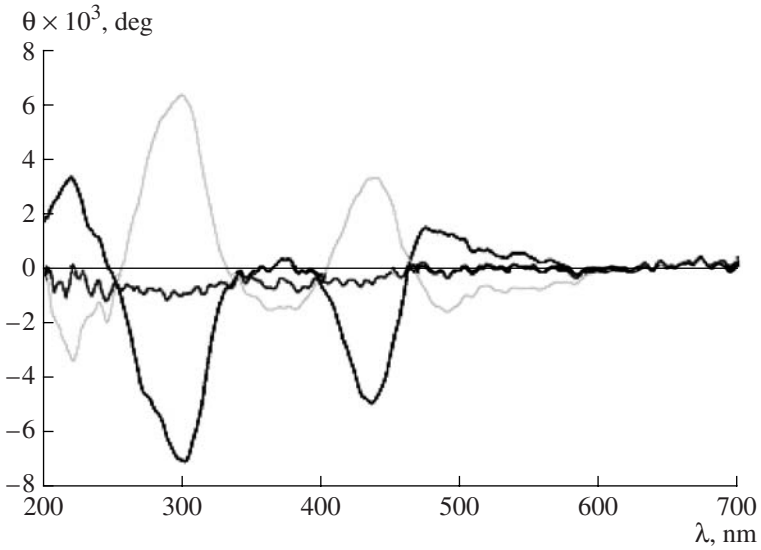

Fig. 12. CD spectra of CdS nanoparticles with the enantiomers of penicillamine as ligands.

and emission by nanoparticles depend on the particle size and shape. The latter in turn depends on the conditions of their synthesis. In connection with this, it is especially interesting whether (and to which degree) the Cotton effects in the CD spectra undergo the respective changes. Perhaps, ICD can provide additional information on the size of nanoparticles. It would be extremely interesting to obtain chiral polarization of their luminescence (i.e., optical activity of emitted light). This is very important in the light of promising use of both organic and inorganic nanoparticles as biosensors. One can expect that investigations of the chiroptical properties of supramolecular complexes of nanoparticles with biomolecules will be shortly substantially extended; in particular, data on chiral induction under the action of proteins will be reported. In the area of catalysis, the use of asymmetric metal catalysts based on enantiomeric carbon nanotubes is most obvious.

ACKNOWLEDGMENTS

This review was supported by the Division of Chemistry and Materials Science of the Russian Academy of Sciences (Program no. 1).

REFERENCES

1. Dresselhaus, M.S., Dresselhaus, G., and Eklund, P., *Science of Fullerene and Nanotubes*, San Diego: Academic, 1996, p. 965.
2. Sergeev, G.B., *Nanokhimiya* (Nanochemistry), Moscow: Mosk. Gos. Univ., 2003.
3. *Nanoparticles: From Theory to Application*, Schmid, G., Ed., Weinheim: Wiley, 2004.
4. Dresselhaus, M.S., Dresselhaus, G., and Saito, R., *Carbon*, 1995, vol. 33, p. 833.
5. Velluz, L. Legrand, M., and Grosjean, M., *Optical Circular Dichroism*, New York: Academic, 1965.
6. Nafie, L.A., *Ann. Rev. Phys. Chem.*, 1997, vol. 48, p. 357.
7. Barron, L.D., *Molecular Light Scattering and Optical Activity*, Cambridge (UK): Cambridge Univ., 2004.
8. Vul', A.Ya. and Sokolov, V.I., *Ros. Nanotekhnologii*, 2007, vol. 3, nos. 3–4, p. 8.
9. Buriak, J.M., *Angew. Chem., Int. Ed. Engl.*, 2001, vol. 40, p. 532.
10. Mason, W.R., *Magnetic Circular Dichroism Spectroscopy,* London: Wiley, 2007.
11. Sokolov, V.I., *Zh. Org. Khim.,* 1999, vol. 35, p. 1289.
12. Polavarapu, P.L., He, J., Crassous, J., and Ruud, K., *ChemPhysChem*, 2005, vol. 6, p. 2535.
13. Krykunov, M., Kundrat, M.D., and Autschbach, J., *J. Chem. Phys.*, 2006, vol. 125, p. 194110.
14. Marconi, G., *The Spectrum*, Ohio (USA): Bowling Green State Univ., 1996, vol. 9, p. 15.
15. Yoshida, Z., Tanekuma, H., Tanekuma, S., et al., *Angew. Chem., Int. Ed. Engl.*, 1994, vol. 73, p. 1597.
16. Belgorodsky, B., Fadeev, L., Kolsenik, J., et al., *ChemBioChem*, 2006, vol. 7, p. 1783.
17. Ohsawa, S., Maeda, K., and Yashima, E., *Macromolecules*, 2007, vol. 40, p. 9244.
18. Bashilov, V.V., Petrovskii, P.V., and Sokolov, V.I., *Izv. Akad. Nauk, Ser. Khim.*, 1993, no. 2, p. 428.
19. Bashilov, V.V., Petrovskii, P.V., Sokolov, V.I., et al., *Izv. Akad. Nauk, Ser. Khim.*, 1996, no. 5, p. 1268.
20. Sokolov, V.I. and Bashilov, V.V., *Platinum Met. Rev.*, 1998, vol. 48, p. 18.
21. Song, L.C., Liu, P.C., Liu, J.T., et al., *Eur. J. Inorg. Chem.,* 2003, no. 17, p. 3201.
22. Zhang, H., Zhu, C.F., Li, L., et al., *Chin. Chem. Lett.,* 2004, vol. 15, p. 1411.
23. Bashilov, V.V., Dolgushin, F.M., Sokolov, V.I., et al., *J. Organomet. Chem.*, 2005, vol. 690, no. 19, p. 4330.
24. Abramova, N.V., Ginzburg, A.G., Peregudov, A.S., et al., *Izv. Akad. Nauk, Ser. Khim.,* 2008, no. 9, p. 1932.
25. Suprunovich, S.V., Ginzburg, A.G., and Sokolov, V.I., *Izv. Akad. Nauk, Ser. Khim.*, 1996, no. 4, p. 971.
26. Suprunovich, S.V., Loim, N.M., Dolgushin, F.M., et al., *Izv. Akad. Nauk, Ser. Khim.*, 1997, no. 1, p. 158.
27. Sokolov, V.I., Bashilov, V.V., Abramova, N.V., et al., *Izv. Akad. Nauk, Ser. Khim.*, 2009, no. 3, p. 550.
28. Milukov, V.A., Sinyashin, O.G., Sokolov, V.I., et al., *J. Organomet. Chem.*, 1995, vol. 493, p. 221.
29. Endo, M., Iijima, S., and Dresselhaus, M.S., *Carbon Nanotubes*, Amsterdam: Elsevier, 1997.
30. Ivanovskii, A.L., *Kvantovaya khimiya v materialovedenii. Nanotubulyarnye formy veshchestva* (Quantum Chemistry in Materials Science. Nanotubular Forms of Matter), Yekaterinburg: IKhTT UrO RAN, 1999.
31. Rakov, E.G., Khimiya i primenenie uglerodnykh nanotrubok, *Usp. Khim.*, 2001, vol. 70, no. 10, p. 925.
32. Zakharova, G.S., Volkov, V.L., Ivanovskaya, V.V., and Ivanovskii, A.L., *Nanotrubki i rodstvennye nanostruktury oksidov metallov* (Nanotubes and Related Structures of Metal Oxides), Yekaterinburg: IKhTT UrO RAN, 2005.
33. Dukovic, G., Balaz, M., Doak, P., et al., *J. Am. Chem. Soc.*, 2006, vol. 126, p. 9004.
34. Peng, Z.X., Komatsu, N., Bhattacharya, S., et al., *Nat. Nanotechnol.*, 2007, vol. 2, p. 361.
35. Peng, X., Komatsu, N., Kimura, T., et al., *J. Am. Chem. Soc.*, 2007, vol. 129, p. 15947.
36. Schmid, G., *Struct. Bond*, 1985, vol. 62, p. 51.
37. Mednikov, E.G., Ivanov, S.A., Slovokhotova, I.V., et al., *Angew. Chem., Int. Ed. Engl.*, 2005, vol. 44, p. 6848.
38. Sokolov, A.A., Ternov, I.M., and Zhukovskii, V.Ch., *Kvantovaya Mekhanika* (Quantum Mechanics), Moscow: Nauka, 1979.
39. Gubin, S.P., Kataeva, N.A., and Yurkov, G.Yu., *Nanochastitsy blagorodnykh metallov i materialy na ikh osnove* (Nanoparticles of Noble Metals and Materials Based on Them), Moscow: Azbuka-2000, 2006.
40. Cushing, B.L., Kolesnichenko, V.L., and O'Connor, C.J., *Chem. Rev.*, 2004, vol. 104, no. 9, p. 3893.
41. *Clusters and Colloids from Theory to Applications*, Schmid, G., Ed., Weinheim (Germany): VCH, 1994.
42. Wetzel, T.L. and DePristo, A.E., *J. Chem. Phys.*, 1996, vol. 105, p. 572.
43. Parks, E.K., Kerns, K.P., and Riley, S.J., *J. Chem. Phys.*, 1998, vol. 10, p. C. 10207.
44. Garzón, I.L., Beltran, M.R., Gonzalez, G., et al., *Eur. Phys. J., D,* 2003, vol. 24, p. 105.
45. Garzón, I.L., Reyes-Nava, J.A., Rodríguez-Hernández, J.I., et al., *Phys. Rev., B*, 2002, vol. 66, p. 73403.
46. Goldsmith, M.R., George, C.B., Zuber, G., et al., *Phys. Chem. Chem. Phys.*, 2006, vol. 8, p. 63.
47. Brust, M., Walker, M., Bethell, D., et al., *J. Chem. Soc., Chem. Commun.*, 1994, p. 801.
48. Schaaff, T.G., Knight, G., Shafigullin, M.N., et al., *J. Phys. Chem., B*, 1998, vol. 102, p. 10643.
49. Schaaff, T.G. and Whetten, R.L., *J. Phys. Chem., B,* 2000, vol. 104, p. 2630.
50. Gautier, C. and Bürgi, T., *Chem. Commun.*, 2005, vol. 43, p. 9393.
51. Gautier, C. and Bürgi, T., *J. Am. Chem. Soc.*, 2006, vol. 128, p. 11079.
52. Yao, H., Miki, K., Nishida, N., et al., *J. Am. Chem. Soc.*, 2005, vol. 127, p. 15536.

53. Gautier, C., Taras, R., Gladiali, S., and Bürgi, T., *Chirality*, 2008, vol. 20, p. 486.
54. Jadzinsky, P.D., Calero, G., Ackerson, C.J., et al., *Science*, 2007, vol. 318, p. 430.
55. Marks, L.D., *Philos. Mag., A*, 1984, vol. 49, p. 81.
56. Walter, M., Akola, J., Lopez-Acevedo, O., et al., *Proc. Natn. Acad. Sci.*, 2008, vol. 105, p. 9157.
57. Gautier, C. and Bürgi, T., *J. Am. Chem. Soc.*, 2006, vol. 128, p. 7077.
58. Nishida, N., Yao, H., and Kimura, K., *Langmuir*, 2008, vol. 24, p. 2759.
59. Shemer, G., Krichevski, O., Markovich, G., et al., *J. Am. Chem. Soc.*, 2006, vol. 128, p. 11006.
60. Alvarez, M.M., Khouri, J.T., Schaaff, T.G., et al., *J. Phys. Chem., B*, 1997, vol. 101, p. 3706.
61. Brown, K.R., Walter, D.G., and Natan, M.G., *Chem. Mater.*, 2000, vol. 12, p. 306.
62. Reed, M.A., *Sci. Am.*, 1993, vol. 268, p. 118.
63. Brus, L.E., *Chemistry and Physics of Semiconductor Nanocrystals*, Columbia Univ., 2007, p. 33.
64. Moloney, M.P., Gun'ko, Yu.K., and Kelly, J.M., *Chem. Commun.*, 2007, p. 3900.
65. Elliott, S.D., Moloney, M.P., and Gun'ko, Yu.K., *Nano Lett.*, 2008, vol. 8, p. 2452.
66. Yamashita, I., Hayashi, J., and Hara, M., *Chem. Lett.*, 2004, vol. 33, p. 1158.
67. Keiko, Y., Kenji, S., and Yamashita, I., *Chem. Lett.*, 2006, vol. 35, p. 1192.
68. Iwahori, K. and Yamashita, I., *J. Phys., Conference Series*, 2007, vol. 61, p. 492.